http://doi.org/10.35784/iapgos.6769 received: 30.10.2024 | revised: 08.11.2024 | accepted: 14.11.2024 | available online: 21.12.2024

# COMPUTER SIMULATION OF A SUPERCONDUCTING TRANSFORMER SHORT-CIRCUIT

**Leszek Jaroszyński**
Lublin University of Technology, Department of Electrical Engineering and Smart Technologies, Lublin, Poland

***Abstract.*** *High critical temperature superconductor power devices have unique characteristics that reduce energy losses during transmission and distribution of electricity. These superconductors allow for high current density, enabling the construction of smaller, lighter, and more transportable installations. A superconducting transformer can significantly reduce the dynamic effects of the short-circuit current during the initial milliseconds of a fault. High temperature superconductor windings, on the other hand, are relatively lightweight and have a low heat capacity. Despite being cryogenically cooled and managing already limited current, the windings made of second-generation high-temperature superconductor can be vulnerable to thermal damage, which may occur in a relatively short timeframe. A numerical study of a short circuit in a three-phase power system with a 10 MVA 115/16.5 kV superconducting transformer is presented in this paper. The superconducting tape's nonlinear electrical and thermal characteristics, as well as heat buildup in the transformer windings during a short circuit, are all taken into consideration by the transformer model.*

**Keywords**: superconducting transformer, power grid, short-circuit fault, computer simulation

## SYMULACJA KOMPUTEROWA ZWARCIA TRANSFORMATORA NADPRZEWODNIKOWEGO

***Streszczenie.*** *Urządzenia energetyczne zbudowane z wykorzystaniem nadprzewodników wysokotemperaturowych posiadają unikalne właściwości, które umożliwiają minimalizację strat w przesyle i dystrybucji energii elektrycznej. Dzięki dużej gęstości prądu istnieje sposób na budowę mniejszych, lżejszych i łatwiejszych w transporcie instalacji. Podczas zwarcia transformator nadprzewodnikowy jest w stanie znacznie zmniejszyć dynamiczne skutki prądu zwarciowego w ciągu kilku pierwszych milisekund. Jednak uzwojenia oparte na przewodniku pokrytym nadprzewodnikiem wysokotemperaturowym mają bardzo małą masę, a co za tym idzie małą pojemność cieplną. Pomimo chłodzenia kriogenicznego i już ograniczonego prądu, uzwojenie nadprzewodnika wysokotemperaturowego drugiej generacji będzie narażone na uszkodzenia termiczne, których prawdopodobieństwo pojawi się w stosunkowo krótkim czasie. W artykule przedstawiono analizę numeryczną zwarcia w trójfazowym systemie elektroenergetycznym z transformatorem nadprzewodnikowym 10 MVA 115/16,5 kV. Model transformatora uwzględnia nieliniowe właściwości elektryczne i cieplne taśmy nadprzewodnikowej, a także akumulację ciepła w uzwojeniach transformatora podczas zwarcia.*

**Słowa kluczowe**: transformator nadprzewodnikowy, sieć elektroenergetyczna, zwarcie ruchowe, symulacja numeryczna

## Introduction

From a manufacturing and transportation perspective, high-$T_c$ superconducting transformers will be smaller, lighter, and easier to convey than copper winding transformers. Taking into account the environmental aspects, HTS transformers will allow for the reduction of energy losses and the saving of resources. Additionally, these machines do not use flammable transformer oil. One unique feature of superconducting transformers is their ability to reduce short-circuit current. Therefore, these devices can be designed with a low short circuit voltage value, which will translate into lower voltage drops, lower reactive power and higher grid stability [3, 4, 7–9].

In densely urbanized areas, this will make much better use of underground and indoor transformer stations. Furthermore, cryogenic cooling will help to improve operational safety in many cases and allow the use of power conversion units in buildings with strong fire protection limitations.

Windings built on the basis of a normal metal conductor coated with a thin HTS layer (second generation HTS tape) have very low mass and therefore low thermal capacity. Despite cryogenic cooling and the limited short-circuit current, the superconducting winding may be exposed to thermal or dynamic damage. To investigate the phenomena occurring during a short circuit in a power system, numerical analysis may prove to be useful. A commonly used tool for numerical analysis of field phenomena is the finite element method (FEM). This advanced concept of approximate solving of systems of algebraic or differential equations is based on dividing the analyzed domain into a finite number of much smaller basic elements. For objects with a large geometric aspect ratio, such as the 2G HTS tape, the necessary domain discretization creates a huge numerical problem, the solution of which in some cases exceeds computer resources.

Analysis of superconducting elements based on circuit simulators like SPICE allows for minimizing computational costs while maintaining the usability of results. It does not consider the distribution of the electromagnetic field in the machine, but focuses on solving nonlinear differential equations to determine quantities such as voltage, current or temperature. This excludes its use in some cases (e.g. AC loss simulation), but at the same time predisposes to the study of transient states in a superconducting device working in an electrical grid [1, 5].

This paper presents a numerical analysis of short circuit failures in a three-phase power system with a 10 MVA 115/16.5 kV "wye-delta" superconducting transformer. Additional analysis of a copper winding transformer was used to verify the presented approach.

## 1. Computer model of HTS coated conductor

The nonlinear resistance of the yttrium superconductor layer $R_{HTS}$ can be derived from Rhyner's power law equation:

$$R_{HTS}(T,B) = \frac{E_c L}{I_c(T,B)} \left( \frac{I}{I_c(T,B)} \right)^{n_R(T,B)-1} \tag{1}$$

where: $I$ – current in HTS layer, $L$ – length of HTS tape, $E_c$ – constant (1 μV/cm for HTS), $I_c$ – tape critical current as the function of temperature $T$ and magnetic flux density $B$, $n_R$ – Rhyner's exponent $B$ and $T$ dependent.

Neglecting the influence of the magnetic field, the equations for the critical current and Rhyner's exponent can be written as:

$$I_c(T) = \begin{cases} I_{c0} \left( \dfrac{T_c - T}{T_c - T_0} \right)^{\beta} & T < T_c \\ 0 & T \geq T_c \end{cases} \tag{2}$$

$$n_R(T) = n_{R0} \frac{T_0}{T} \tag{3}$$

where: $T_c$ – critical temperature of HTS, $I_{c0}$ – critical current in temperature $T_0$, $n_{R0}$ – power law exponent in temperature $T_0$, $\beta$ – constant specific for HTS material [2].

A linear model was adopted to describe the resistance $R_m$ of the normal metal layer of the HTS tape (Hastelloy, silver, copper):

$$R_m(T) = (a_m T + b_m) \frac{L}{d_m \cdot w} \tag{4}$$

where: $a_m$, $b_m$ – constants, $d_m$ – metal layer thickness, $w$ – HTS coated conductor width.

The SPICE code describing the HTS coated conductor tape is shown in Listing 1. The essential coefficients are embedded in the code, others can be found in [5] and [11].

*Listing 1. SPICE code for 2G HTS tape*

```
.SUBCKT tapeHTS IN1 IN2 T PARAMS:
+ L=1 w=4e-3 aCu=6.89e-11 bCu=-3.3036e-9 dCu=40e-6
+ aAg=6.0561e-11 bAg=-1.863214e-9 dAg=3.8e-6
+ aH=0 bH=1.25e-6 dH=50e-6
+ Rres=1e-18 Ic0=110 n0=20 Tc=92 T0=77 beta=1.5 Ec=1e-4
* normal metal layers Cu, Ag, C-276 (H)
GCu IN1 IN2 VALUE {
+ (V(IN1)-V(IN2))/(aCu*V(T)+bCu)/L*(w*dCu)}
GAg IN1 IN2 VALUE {
+ (V(IN1)-V(IN2))/(aAg*V(T)+bAg)/L*(w*dAg)}
GH IN1 IN2 VALUE {(V(IN1)-V(IN2))/(aH*V(T)+bH)/L*(w*dH)}
* HTS layer
GHTS IN1 1 VALUE {
+ (V(IN1)-V(IN2))/(Rres+V(Rc)*PWR((I(V1))/V(Ic),V(n)-1))}
V1 1 IN2 0
E1 Ic 0 VALUE {
+ LIMIT(Ic0*PWRS((Tc-V(T))/(Tc-T0),beta), 1e-3, 1e6)}
E2 Rc 0 VALUE {Ec*L/V(Ic)}
E3 n 0 VALUE {LIMIT(n0*T0/V(T), n0*T0/Tc, 1e6)}
R1 IN1 IN2 1G
R2 Ic 0 1k
R3 Rc 0 1k
R4 n 0 1k
.ENDS tapeHTS
```

The temperature $T$ of the superconducting tape is calculated using the equivalent circuit of thermal phenomena shown in the Figure 1.

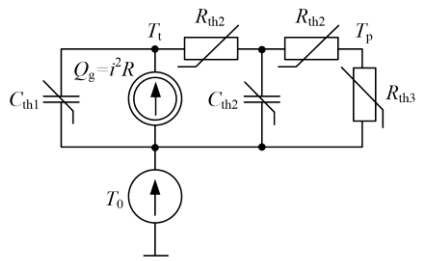


*Fig. 1. Equivalent electrical circuit of thermal phenomena for an insulated HTS tape cooled in a cryogenic bath: $Q_g$ – heat generated in tape fragment, $C_{th1}$ – tape thermal capacity, $C_{th2}$ – insulation thermal capacity, $R_{th2}$ – insulation thermal resistance, $R_{th3}$ – thermal resistance representing heat transferred to refrigerant*

This simplified model takes into account the heat capacity of the tape and the insulation, the thermal resistance of the insulation, and the nonlinear heat transfer characteristics of the liquid nitrogen bath. The heat flux density characteristics of the liquid nitrogen are recorded in the Table 1 [5].

*Table 1. Heat flux density linearization parameters for liquid nitrogen*

| temperature difference | heat flux density, W/m$^2$ |
|---|---|
| $0 \le \Delta T \le 2$ K | $1550 \cdot \Delta T$ |
| $2 < \Delta T \le 11$ K | $15767 \cdot \Delta T - 28433$ |
| $11 < \Delta T \le 19$ K | 145000 |
| $19 < \Delta T \le 33$ K | $-9928.6 \cdot \Delta T + 333643$ |
| $\Delta T > 33$ K | $81.7 \cdot \Delta T + 3304$ |

## 2. Transformer model

The three-phase transformer model is based on a typical description using a system of equations (5), where: subscript numbers 1 or 2 refer to primary or secondary winding, subscript letters a, b and c denote transformer phases, $n$ is the number of winding turns, $\phi$ is magnetic flux in the core limb (column). It takes into account winding resistances $R$, stray magnetic flux inductances $L_s$, and a three-column so-called warm magnetic core (nonlinear reluctances $R_\mu$, Jiles-Atherton magnetic hysteresis model). The magnetization curve of the core material corresponds to a cold rolled grain oriented sheets with a maximum flux density of 1.75 T and a thickness of 0.27 mm operating at room temperature. Equivalent circuit of no-load state of "wye-delta" transformer is shown in Figure 2a and Figure 2b.

Using this transformer model it is possible to simulate a three-phase devices with copper, HTS or mixed windings by selecting appropriate sub-circuits and the corresponding sets of numerical coefficients [5, 11].

$$\begin{cases} u_{1a} = i_{1a}R_{1a} + L_{s1}\dfrac{\mathrm{d}i_{1a}}{\mathrm{d}t} + n_1\dfrac{\mathrm{d}\phi_a}{\mathrm{d}t} \\ u_{1b} = i_{1b}R_{1b} + L_{s1}\dfrac{\mathrm{d}i_{1b}}{\mathrm{d}t} + n_1\dfrac{\mathrm{d}\phi_b}{\mathrm{d}t} \\ u_{1c} = i_{1c}R_{1c} + L_{s1}\dfrac{\mathrm{d}i_{1c}}{\mathrm{d}t} + n_1\dfrac{\mathrm{d}\phi_c}{\mathrm{d}t} \\ i_{1a} + i_{1b} + i_{1c} + i_n = 0 \\ n_2\dfrac{\mathrm{d}\phi_a}{\mathrm{d}t} = i_{2a}R_{2a} + L_{s2}\dfrac{\mathrm{d}i_{2a}}{\mathrm{d}t} + u_{2a} \\ n_2\dfrac{\mathrm{d}\phi_b}{\mathrm{d}t} = i_{2b}R_{2b} + L_{s2}\dfrac{\mathrm{d}i_{2b}}{\mathrm{d}t} + u_{2b} \\ n_2\dfrac{\mathrm{d}\phi_c}{\mathrm{d}t} = i_{2c}R_{2c} + L_{s2}\dfrac{\mathrm{d}i_{2c}}{\mathrm{d}t} + u_{2c} \\ u_{2a} + u_{2b} + u_{2c} = 0 \\ n_1 i_{1a} - n_2 i_{2a} - \phi_a R_{\mu a} - n_1 i_{1b} + n_2 i_{2b} + \phi_b R_{\mu b} = 0 \\ n_1 i_{1b} - n_2 i_{2b} - \phi_b R_{\mu b} - n_1 i_{1c} + n_2 i_{2c} + \phi_c R_{\mu c} = 0 \\ \phi_a + \phi_b + \phi_c = 0 \end{cases} \quad (5)$$

The basic parameters of a copper winding transformer are summarized in Table 2. A superconducting transformer with the same power and rated voltages is described by the selected values shown in Table 3. It should be noted that the HTS transformer is designed for the same power and voltages, however with a much lower short-circuit voltage than the conventional transformer (4.1% vs. 8%).

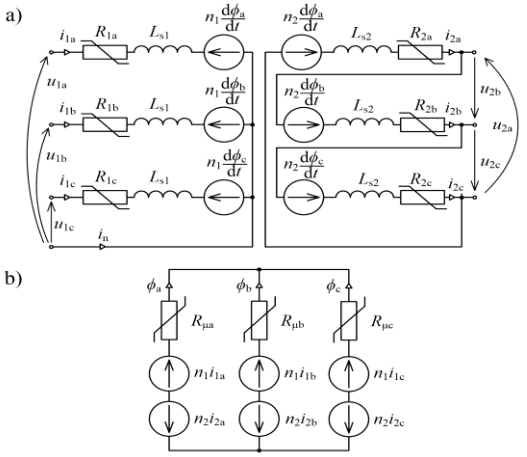


*Fig. 2. Equivalent circuit of "wye-delta" superconducting transformer (a), the simplified equivalent circuit of magnetic phenomena in three-legged three-phase transformer (b)*

*Table 2. Basic simulation parameters of conventional transformer (copper windings)*

| parameter | value |
|---|---|
| nominal power $S_n$ | 10 MVA |
| nominal voltages $U_{1n}/U_{2n}$ | 115 kV/16.5 kV |
| load loss $\Delta P_m$ | 73.41 kW |
| short circuit voltage $U_{z\%}$ | 8% |
| correction factor $k_{zT}$ | 0.997 |
| short circuit resistance $R_{zT}$ | 9.7 Ω |
| short circuit reactance $X_{zT}$ | 105.5 Ω |
| short circuit impedance $\underline{Z}_k$ at the fault location | (0.20+2.26i) Ω |

*Table 3. Selected simulation parameters of the superconducting transformer*

| parameter | value |
|---|---|
| short circuit voltage Uz% | 4.1% |
| transformer correction factor kzT | 1.02 |
| short circuit resistance RzTsc (superconducting state @77K) | 0.1 Ω |
| short circuit resistance RzTr (resistive state @77 K) | 42.2 Ω |
| short circuit reactance XzT | 55.3 Ω |
| short circuit impedance Zksc (superconducting state @77 K) | (0.002+1.236i) Ω |
| short circuit impedance Zkr (resistive state @77 K) | (0.869+1.236i) Ω |

## 3. Short-circuit simulation

The computer simulation of short circuits on the secondary side of a transformer Tr connected to the power grid *Q* was performed (Figure 3a). Basic parameters of the power grid *Q* are shown in Table 4. The simulation results were compared with simplified calculations of the short-circuit faults [6] performed for the scheme shown in the Figure 3b.

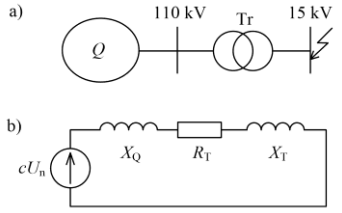


*Fig. 3. Superconducting transformer Tr connected to the power grid Q (a), equivalent circuit for simplified calculation of the short circuit (b): c – voltage factor of the power grid, $U_n$ – system nominal voltage, $X_Q$ – grid equivalent reactance, $R_T$ – transformer equivalent resistance, $X_T$ – transformer equivalent reactance*

*Table 4. Simulation parameters of the power system Q*

| parameter | value |
|---|---|
| nominal grid voltage $U_n$ | 110 kV |
| system short circuit power $S''_k$ | 2800 MVA |
| system voltage factor $c$ | 1.1 |
| system reactance $X_Q$ | 4.73 Ω |

In each case analyzed further, the fault was triggered for the worst-case scenario – when the supply $u_{AB}$ voltage was crossing zero (at time $t$ = 138.3 ms on the following graphs).

### 3.1. Symmetric short-circuit

A symmetrical short circuit (three-phase) analysis was performed for the transformer with copper windings. Simulation was made assuming no heat exchange between windings and transformer oil. Due to the high values and relatively short duration of fault currents, such simplification leads to results with practically insignificant errors. The temperature increase of the secondary windings and the secondary current waveforms for the conventional transformer are shown in the Figure 4.

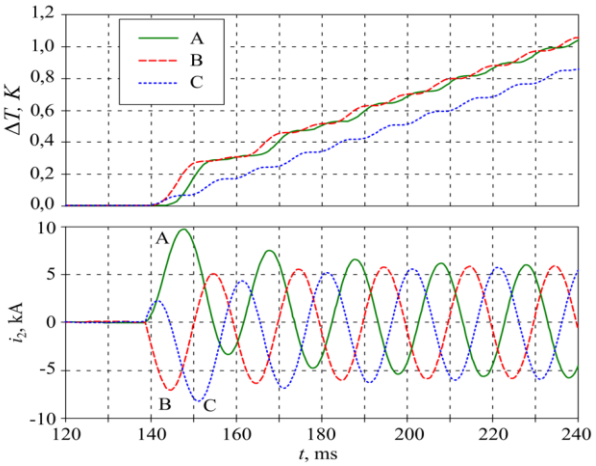


*Fig. 4. Copper winding transformer symmetric short circuit: winding temperature change (upper plot), current at the fault location (lower plot)*

Massive copper windings (2117 kg) are characterized by high thermal capacity. Despite peak current of almost 10 kA, small temperature rise indicates high thermal endurance of such a machine – a short circuit lasting two seconds causes the temperature of the windings to increase by approximately 20 K.

The comparison of the results obtained by the approximate calculation method and the results of computer simulation carried out for two initial temperatures are presented in the Table 5. These results remain in relatively good agreement.

Similar analysis was performed for the transformer with the windings made of HTS coated conductors. The temperature increase of the HTS windings is shown in Figure 5 and the secondary current waveforms in Figure 6.

*Table 5. Calculation results compared with the computer simulation outcomes (copper winding transformer, symmetric short-circuit)*

| parameter | value | | |
|---|---|---|---|
| | calculation | SPICE | |
| | | $T_0$=293 K | $T_0$=348 K |
| initial current $I''_k$ | 4.20 kA | 4.15 kA | 4.14 kA |
| current factor $k$ | 1.77 | 1.66 | 1.63 |
| peak current $i_p$ | 10.52 kA | 9.75 kA | 9.57 kA |

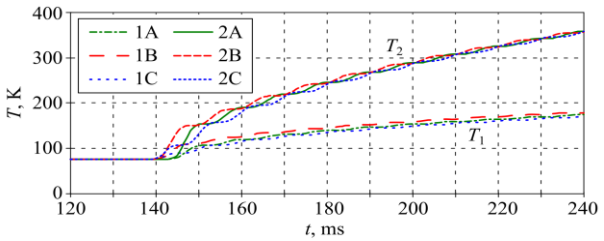


*Fig. 5. Winding temperatures during symmetric short circuit of the superconducting transformer (1A, 1B, 1C – primary windings, 2A, 2B, 2C – secondary windings)*

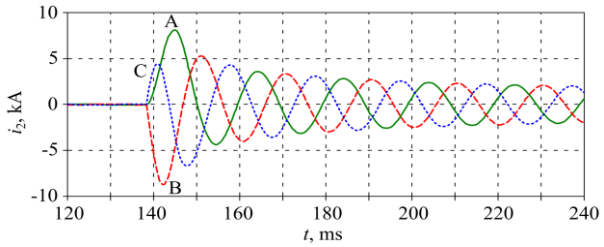


*Fig. 6. Currents at the fault location during symmetric short circuit of the superconducting winding transformer (A, B, C – circuit phases)*

The HTS transformer is capable of limiting the short-circuit current. Despite the low short circuit voltage ($U_{z\%}$ = 4.1%). The peak and steady currents are lower than those of the conventional transformer ($U_{z\%}$ = 8%). HTS tape in one transformer phase weighs only 35 kg, and consequently the temperature increase of the secondary HTS windings is very dynamic, which can lead to damage of the superconducting tape in 100 ms. Short-circuit protection system with a very short fault detection and activation time is necessary.

The comparison between the approximate calculation method and the computer simulation results shown in Table 6 may need some explanation.

*Table 6. Calculations vs. simulation results (HTS transformer, symmetric fault)*

| parameter | value | | |
|---|---|---|---|
| | calculation | | SPICE |
| | SC state | resistive state | |
| initial current $I''_k$ | 7.71 kA | 6.31 kA | 7.71 kA |
| current factor $k$ | 1.99 | 1.14 | - |
| peak current $i_p$ | 21.75 kA | 10.16 kA | 8.74 kA |

The influence of the superconductor state on the calculation result presented above is significant. Using the HTS tape parameters specific to the superconducting state (SC state) for calculations leads to an overestimation of the peak current value. The use of HTS tape parameters specific to the resistive state at liquid nitrogen temperature (77 K) gives results similar to those of computer simulation. The higher current value is due to the fact that the simplified calculation method does not take into account the rapid changes in the superconductor parameters within the first milliseconds after the fault occurs.

### 3.2. Asymmetric short-circuit

The second analyzed case was an asymmetric short-circuit (two-phase) of wires A and B initiated at the same moment as before. Current waveforms for the HTS transformer during the short circuit are shown in Figure 7.

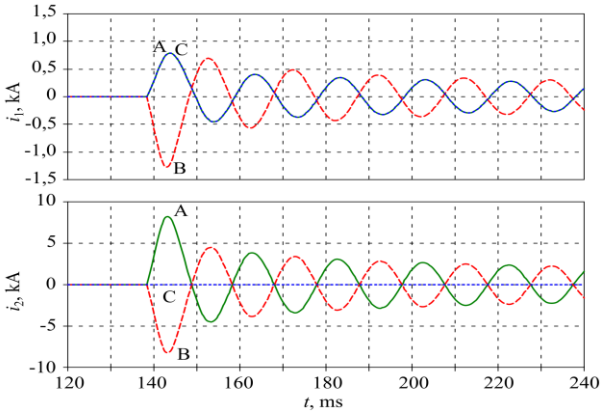


*Fig. 7. Waveforms in the course of the asymmetric short circuit of the HTS winding transformer: primary currents (upper plot), currents at the fault location (lower plot)*

Similarly to the symmetric short circuit, a very rapid decay of the aperiodic component of the fault current and a clear limitation of the periodic component by the increasing winding resistance can be observed.

Winding temperature evolution is shown in Figure 8. During the asymmetric short circuit (wires A and B) of Yd11 transformer, the secondary winding in phase B is subject to the highest thermal load, and reaches 346 K in the analyzed time.

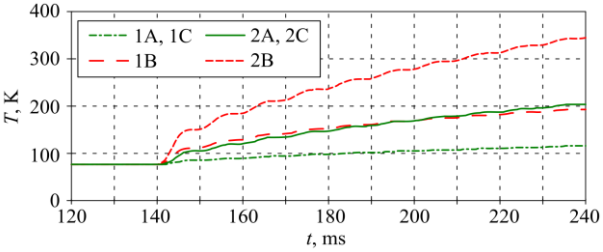


*Fig. 8. Winding temperatures during asymmetric short circuit of the superconducting transformer: 1A, 1B, 1C – primary windings, 2A, 2B, 2C – secondary windings*

The evolution of winding resistances and the short-circuit time constant during asymmetric fault of the superconducting transformer are depicted in Figure 9.

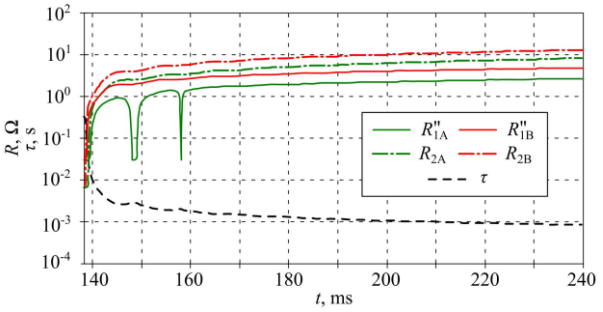


*Fig. 9. Winding resistances and the circuit time constant during asymmetric short circuit of the superconducting transformer (" – value related to the secondary side)*

As in the case of symmetric fault, the short-circuit time constant $\tau$ decreases from 300 ms to approximately 1 ms during the first 100 ms, which results in a very rapid decay of the aperiodic component of the current.

Again, the use of parameters specific to the resistive state of HTS tape at liquid nitrogen temperature gives the calculated peak current similar to those of computer simulation (Table 7).

*Table 7. Calculations vs. simulation results (HTS transformer, asymmetric fault)*

| parameter | value | | |
|---|---|---|---|
| | calculation | | SPICE |
| | SC state | resistive state | |
| initial current $I''_k$ | 6.68 kA | 5.46 kA | 6.68 kA |
| current factor $k$ | 1.99 | 1.14 | - |
| peak current $i_p$ | 18.83 kA | 8.00 kA | 8.20 kA |

## 4. Conclusion

During a short-circuit failure, the superconducting transformer can minimize the peak value and therefore the dynamic impact of the short-circuit current in a matter of milliseconds.

On the other hand, windings made of a high-$T_c$ superconductor coated conductor have a very low mass and, as a result, low heat capacity. Despite cryogenic cooling and already limited current, the second generation high temperature superconductor winding will be subjected to thermal degradation, which is likely to occur within a few dozen milliseconds. Therefore, HTS transformer with liquid nitrogen-cooled windings requires cooperation with a special protection system with an suitably short detection and switch-off time. To improve the short-circuit resilience of superconducting windings, they can be reinforced with a parallel stainless steel tape [10]. Another solution seems to be the production of HTS tapes with an alloy substrate of a specifically designed thickness much greater than those available on the market of second generation superconducting tapes.

Based on the computer simulation of the HTS transformer, it is possible to conclude that the appropriate method for assessing a short circuit fault in such a machine is to calculate the peak current and the initial short circuit current, taking into account the resistivity of the normal metal layers of the winding tape at cryogenic coolant temperature.

## References

[1] Czerwinski D. et al.: Comparison of Overcurrent Responses of 2G HTS Tapes. IEEE Transactions on Applied Superconductivity 26(3), 2016, 1–4.
[2] Grilli F. et al.: Computation of Losses in HTS Under the Action of Varying Magnetic Fields and Currents. IEEE Transaction on Applied Superconductivity 24(1), 2014, 78–110.
[3] Irannezhad F., Heydari H.: Conducting a Survey of Research on High Temperature Superconducting Transformers. IEEE Transactions on Applied Superconductivity 30(6), 2020, 1–13.
[4] Janowski T., Wojtasiewicz G., Jaroszyński L.: Transformatory nadprzewodnikowe. Wydawnictwo Książkowe Instytutu Elektrotechniki, Warszawa 2016.
[5] Jaroszyński L., Wojtasiewicz G., Janowski T.: Considerations of 2G HTS transformer temperature during short circuit. IEEE Transactions on Applied Superconductivity 28(4), 2018, 1–5.
[6] Kacejko P., Machowski J.: Zwarcia w systemach elektroenergetycznych. WNT, Warszawa 2018.
[7] Kalsi S. S.: High temperature superconductors to electric power equipment. IEEE Press. Wiley, Hoboken, New Jersey 2011.
[8] Marchionini B. G. et al.: High-Temperature Superconductivity: A Roadmap for Electric Power Sector Applications. IEEE Transaction on Applied Superconductivity 27(4), 2017, 1–7.
[9] Noe M.: Superconducting Transformers. EUCAS 2017 Short Courses: Superconducting Power Applications. Switzerland, Geneva, 2017.
[10] Pi W. et al.: Fault Current Characteristics of Parallel Stainless Steel & REBCO Tapes and a 6 kV/400 V HTS Transformer. IEEE Transaction on Applied Superconductivity 31(5), 2021, 1–6.
[11] Surdacki P., Jaroszyński L., Woźniak Ł.: Modelling short-circuit current of a 21 MVA HTS superconducting transformer. Journal of Physics: Conference Series 1782, 2021, 012036.

**Ph.D. Leszek Jaroszyński**
e-mail: l.jaroszynski@pollub.pl

He received the Ph.D. in electrical engineering from Faculty of Electrical Engineering and Computer Science, Lublin University of Technology, Lublin, Poland in 2000. He works as an assistant professor in the same faculty's Department of Electrical Engineering and Smart Technologies. His research interests include: computer analysis of non-linear electromagnetic systems, non-thermal plasma and superconducting devices, applied superconductivity.

https://orcid.org/ 0000-0003-1674-0970